

# Homodyne detection of a two-photon resonance assisted by cooperative emission

Chetan Sriram Madasu<sup>1</sup>, Chang Chi Kwong<sup>1,2</sup>, David Wilkowski<sup>1,2,3,4</sup> and Kanhaiya Pandey<sup>5</sup>

<sup>1</sup> Quantum Hub, Division of Physics and Applied Physics, Nanyang Technological University, 21 Nanyang Link, 637371 Singapore

<sup>2</sup> MajuLab, CNRS-UCA-SU-NUS-NTU International Joint Research Unit, Singapore

<sup>3</sup> Centre for Quantum Technologies, National University of Singapore, 3 Science Drive 2, 117543 Singapore

<sup>4</sup> Centre for Disruptive Photonic Technologies, The Photonics Institute, Nanyang Technological University, Singapore 637371, Singapore

<sup>5</sup> Department of Physics, Indian Institute of Technology Guwahati, Guwahati, Assam 781039, India

E-mail: david.wilkowski@ntu.edu.sg, kanhaiyapandey@iitg.ac.in

May 2, 2022

**Abstract.** Using a transient regime approach, we explore atomic two-photon spectroscopy with self-aligned homodyne interferometry in the  $\Lambda$ -system. The two light sources at the origin of the interference, are the single-photon transient transmission of the probe, and the slow light of the electromagnetically induced transparency, whereas the atomic medium is characterized by a large optical depth. After an abrupt switch off of the probe laser (flash effect), the transmission signal is reinforced by cooperativity, showing enhanced sensitivity to the two-photon frequency detuning. If the probe laser is periodically switched on and off, the amplitude of the transmission signal varies and remains large even at high modulation frequency. This technique has potential applications in sensing, such as magnetometry and velocimetry, and in coherent population trapping clock.

**Keywords :** electromagnetically induced transparency, atomic coherence, interference, optical transient phenomena, two-photon spectroscopy

Submitted to: *New Journal of Physics*

## 1. Introduction

Since the first experimental evidences of coherent population trapping (CPT) [1] and electromagnetically induced transparency (EIT) [2], the narrow dark two-photon resonance [3] has been a key feature for many fundamental and practical phenomena. Without being exhaustive, we point out: slowing and storage of light [4, 5], quantum memory [6, 7], CPT clock [8, 9, 10, 11, 12, 13], microwave and terahertz generation and detection [14, 15, 16, 17], laser cooling [18, 19], Raman velocimetry [20], and nonlinear phenomena and many-body photonics systems [21, 22, 23, 24]. A generalization of CPT involving dark multi-photon resonances has been also demonstrated recently [25]. Improvement in the precision of the two-photon resonance can be achieved using cooperative effect, for example, by embedding the atomic medium into an optical resonator [26]. In particular, linewidth of *bad* cavities have been significantly narrowed down [27, 28, 29, 30]. Without cavities, EIT resonances are narrowed down using medium with large single-photon optical depth (OD) [31, 32]. Here, the two-photon resonance linewidth is inversely proportional to the OD of the medium, the cooperativity parameter.

In this paper, we propose a new method to measure the two-photon detuning using cooperative effect in a dilute EIT medium with large OD. We abruptly switch off or perform a square pulse modulation of the probe beam (see Fig. 1a), leading to two major improvements over above mentioned techniques. First, cooperativity can further enhance the transient signal as observed in *flash* experiments [33]. Second, the difference in time scales in the atomic system naturally leads to a high repetition rate homodyne interference between the transient transmitted field component coming from the single-photon response of the medium and the EIT slow light field. Since these two fields share the same electromagnetic mode, the homodyne interference is self-aligned in space. We note that pulsed techniques were already considered in CPT clock either in Ramsey-type configurations [34, 35, 36, 37], or with periodic pulse sequences [38]. However, in these configurations both the probe and control laser beams are modulated, and do not lead to a homodyne interference in the transmitted field.

## 2. Model and Results

We now describe the model and the assumptions used in our study. We consider a plane wave probe beam shining on a slab of zero temperature atomic medium with thickness  $L$ . For a weak probe beam below saturation, the transmitted field at time

$t$  is  $E(t) \exp(-i\omega_p t)$ , where the complex amplitude reads [39, 33]

$$E(t) = \frac{1}{2\pi} \int_{-\infty}^{\infty} \tilde{E}_i(\omega) \exp \left[ -\frac{b(\delta)}{2} + i\phi(\delta) \right] e^{-i(\omega - \omega_p)t} d\omega. \quad (1)$$

$\tilde{E}_i(\omega)$  is the Fourier component of the incident field at frequency  $\omega$ ,  $\delta = \omega - (E_2 - E_1)/\hbar$  is the frequency detuning of the Fourier component with respect to the resonance of the probed  $|1\rangle \rightarrow |2\rangle$  transition (see Fig. 1), and  $\omega_p$  is the carrier frequency of the probe beam.  $b(\delta) = \text{Im}\{\chi(\delta)\}kL$  and  $\phi(\delta) = \text{Re}\{\chi(\delta)\}kL/2$  are the OD and the phase shift for an optical field at detuning  $\delta$ , respectively.

### 2.1. Two-level system

As a preliminary study, we consider a two-level system, where  $\chi(\delta) \equiv \chi_{1p}(\delta) = \frac{-6\pi\rho}{k^3} \frac{\gamma_{21}}{2} \left( \delta + \frac{i\gamma_{21}}{2} \right)^{-1}$  is the one-photon susceptibility of the dilute atomic ensemble assuming each atom scatters light independently. Here,  $\gamma_{21}$  is the transition linewidth,  $\rho$  is the number density of the medium, and  $k$  is the wave-number of the optical field. The bulk properties of the medium *i.e.*,  $\rho$  and  $L$ , are encapsulated into a single parameter,  $b_0 \equiv b(0) = \frac{6\pi\rho L}{k^2}$ , which is the resonant single-photon OD. We assume that  $b_0 \gg 1$  and disregard the incoherent multiple scattering field in the forward transmission [40].

At first, the probe beam is turned on abruptly, and shined for a duration long enough for the steady-state regime to be established, before being turned off abruptly (see the black curve in Fig. 1b). Defining  $\delta_p$  as the probe beam carrier detuning, the resonant ( $\delta_p = 0$ ) transmitted intensity,  $I(t) \equiv |E(t)|^2$ , is illustrated by the red curve in Fig. 1b. Two flashes of light are observed. The initial flash (see left inset in Fig. 1b), during probe ignition, corresponds to the Sommerfeld-Brillouin optical (SBO) precursors [41, 42, 39, 43, 44]. During probe extinction, the flash of light is related to the free induction decay (FID) signal [45, 46] (see right inset in Fig. 1b). The flash has a fast cooperative decay time that scales like [47]

$$\tau_f \sim \frac{1}{b_0 \gamma_{21}}. \quad (2)$$

For an optically thick medium,  $\tau_f$  is much shorter than excited state lifetime  $\tau = \gamma_{21}^{-1}$ .

To gain physical insight, we decompose the amplitude of the transmitted field as

$$E(t) = E_i(t) + E_s(t), \quad (3)$$

where,  $E_i(t)$  and  $E_s(t)$  are the amplitudes of the incident and forward scattered fields, respectively, in complex notation. In the steady-state regime,  $E \approx 0$  means that  $E_s \approx -E_i \approx -1$ , i.e. a destructive interference between the incident field and the forward scattered field. Here, we use the normalisation:  $|E_i| = 1$  when the field is on, and the following notation convention: when quantities do not explicitly depend on time, they correspond to the steady-state values. When the incident field is switched off at  $t = 0^+$ , since the atoms has a finite response time,  $E(0^+) \approx E_s \approx -1$  and  $I(0^+) \approx 1$  (see Fig. 1b). As pointed out in Refs. [48, 33], the FID flash is a measurement of  $E_s$ .

The FID flash and SBO precursors in Fig. 1 have the same temporal profile. This can be understood from the temporal version of Babinet principle [49]. For  $\delta_p = 0$  and  $b_0 \gg 1$ , the fields during probe ignition and extinction should sum to zero, i.e., the steady-state transmitted field value [48]. In other words, the FID flash and SBO precursor fields are complementary at resonance, i.e., they have equal amplitudes but opposite signs.

## 2.2. Three-level $\Lambda$ system

We now turn to the case of the  $\Lambda$ -system, with an additional state  $|3\rangle$ . In the presence of a continuous control beam on the transition  $|3\rangle \rightarrow |2\rangle$  ( $\Omega_c \neq 0$ , see Fig. 1c), EIT phenomenon takes place and the susceptibility of the probe beam reads,

$$\chi(\delta) = \chi_{1p}(\delta) \left[ 1 - \frac{|\Omega_c|^2/4}{(\delta + \frac{i\gamma_{21}}{2})(\delta - \delta_c + \frac{i\gamma_{31}}{2})} \right]^{-1}, \quad (4)$$

where  $\gamma_{31}/2$  is the relaxation rate of coherence between the ground states  $|3\rangle$  and  $|1\rangle$ , and  $\delta_c$  is the frequency detuning of the control beam. Since OD is large, the transmission signal weakly depends on  $\delta_c$ , and we set  $\delta_c = 0$ . Therefore,  $\delta_p = 0$  also indicates the two-photon resonance condition. Under this condition, the temporal evolution of the transmitted intensity is shown in Fig. 1c, and can be directly compared to the two-level case of Fig. 1b. A salient difference is the increase of the transmission well after the SBO precursor ( $t \sim -500\gamma_{21}^{-1}$ ), due to the development of the EIT slow light. For  $\gamma_{31} \ll \Omega_c, \gamma_{21}$ , this occurs after a group delay of (See the appendix)

$$\tau_{EIT} = b_0 \frac{\gamma_{21}}{|\Omega_c|^2}. \quad (5)$$

As previously observed with a rubidium cold gas [39], we find an anti-flash at probe extinction, i.e.  $I(0^+) \approx 0$ . To understand the appearance of this

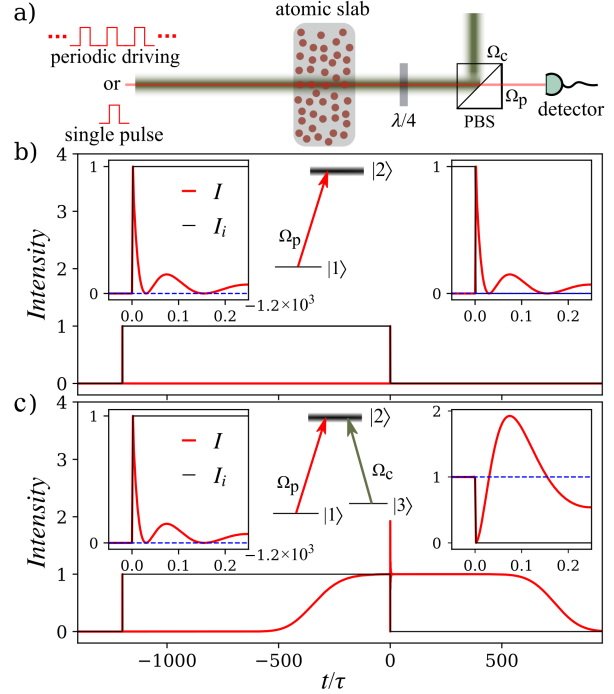


**Figure 1.** (a) Two plane waves, a control beam and a probe beam, are resonantly coupled to a slab of atomic  $\Lambda$ -system. The probe field is abruptly switched off or periodically turned on and off. Its transmitted intensity is measured on a detector. (b&c) Temporal evolution of the probe transmitted intensity (red curve) with a square input pulse (black curve), for  $b_0 = 200$ . The central sketches are energy diagrams and the active optical fields.  $\Omega_c$ , and  $\Omega_p$  are the control field and probe field Rabi frequencies, respectively. The SBO precursors and flashes are shown in the left and right insets, respectively. The dashed blue lines are the intensity levels that the flashes or precursors relax to. (b) Two-level system i.e.,  $\Omega_c = 0$ . (c) Three-level system with  $\Omega_c = \gamma_{21}/2$ ,  $\gamma_{31} = 0$  and  $\delta_c = 0$ .

anti-flash, we consider the following modified field decomposition,

$$E(t) = E_i(t) + E_s(t) + E_{EIT}(t). \quad (6)$$

In addition to the first two right-hand-side terms that are found in the two-level case, a third term is added to include the field of the EIT slow light. There is a physical interest in this new field decomposition, because of the clear time scale separation between the flash and the slow EIT light, i.e.,  $\tau_f \ll \tau_{EIT}$ . The SBO precursors are identical for the two-level and three-level schemes as shown on left insets of Fig. 1b and Fig. 1c, respectively. Indeed, the short time scale of the SBO precursors means that they are governed by the two-level response of the probed transition. By complementary argument, the FID flashes (i.e.,  $E_s$ ) are also identical for the two-level and three-level cases. Hence, the clear difference in the FID flashes time profiles (compare right insets in Fig. 1b and Fig. 1c), solely originates from the interference with the additional  $E_{EIT}$  term. At  $\delta_p = 0$  and  $\gamma_{31} = 0$ , the three-level medium

is transparent in the steady-state regime, meaning  $E \approx 1$ . Since  $E_s \approx -1$  from the two-level case, we have  $E_{EIT} \approx E \approx 1$ . Thus  $E(0^+) \approx E_s + E_{EIT} \approx 0$  during probe extinction, as observed in the right inset of Fig. 1c. This anti-flash results from a destructive interference between the FID flash ( $E_s$ ) and the EIT field ( $E_{EIT}$ ).

The nature of the interference, constructive or destructive during probe extinction, depends upon the steady-state phase difference between  $E_{EIT}$  and  $E_s$ . This reads

$$\Delta\phi = \phi_{EIT} - \phi_s \approx \delta_p \tau_{EIT} - \pi = b_0 \frac{\gamma_{21}}{|\Omega_c|^2} \delta_p - \pi. \quad (7)$$

For a small probe detuning of  $\delta_p \ll \gamma_{21}$ , the phase of  $E_s$  has an approximately constant value of  $\phi_s \approx \pi$ . Neglecting off-resonance absorption inside the transparency window, the fringe maxima (constructive interference) is located at  $\Delta\phi = 0 \pmod{2\pi}$ , i.e.,  $\phi_{EIT} = \pi \pmod{2\pi}$ . This condition gives  $E_{EIT} = E_s = -1$ , and a maximum value of  $I(0^+) = 4$ , according to Eq. (6). The first maxima is located at  $|\delta_p| = \delta_\pi$  where [31],

$$\delta_\pi = \frac{\pi}{b_0} \frac{|\Omega_c|^2}{\gamma_{21}}. \quad (8)$$

The  $b_0^{-1}$  prefactor in Eq. (8) encapsulates the cooperative narrowing of the fringe pattern. We confirm this analysis, by integrating Eq. (1) at  $t = 0^+$  with  $\gamma_{31} = 0$  for various values of  $\delta_p$  and  $b_0$  (see 2D color plot Fig. 2). The detuning at the first bright fringe is well captured by Eq. (8) of  $\delta_\pi$  (black dotted curve), and we clearly observed the enhancement of the phase measurement sensitivity, due to cooperative narrowing of the fringes when  $b_0$  increases.

A section at  $b_0 = 200$  is represented by the light grey curve in Fig. 2. The first maximum does not reach the value of four as predicted, due to the presence of residual absorption when the two-photon resonances condition is not exactly fulfilled. The absorption becomes more important at larger detuning which explains the damping of the fringes. The damping is reinforced, when we include a non-zero relaxation of the ground state coherence, as illustrated for  $\gamma_{31} = \gamma_{21}/1000$  by the light grey dashed curve in Fig. 2. If the temperature of the atomic ensemble is finite, we expect similar results as far as the cooperative characteristic rate  $\tau_f^{-1}$  is larger than the Doppler broadening [50], and the relaxation of the ground state coherence remains small (for example, with buffer gas [51] or anti-reflection coated [52, 53, 54] vapor cells).

We have so far analysed the case of long probe duration where the steady-state regime of EIT

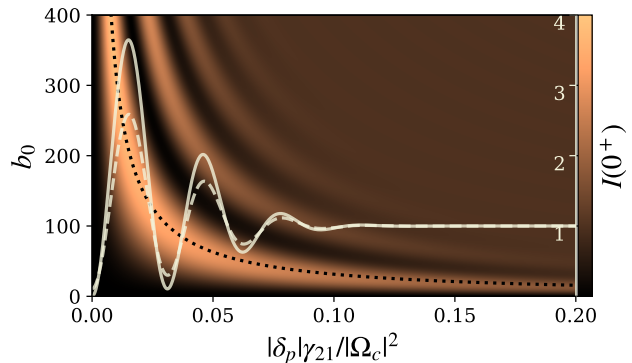


**Figure 2.** Color plot of  $I(0^+)$ , the transmitted intensity at the probe extinction, as function of  $b_0$  (left vertical axis) and the normalized probe detuning for  $\Omega_c = \gamma_{21}/2$ ,  $\delta_c = 0$  and  $\gamma_{31} = 0$ . The dotted black curve represents the first fringe maximum at a probe detuning corresponding to  $\delta_\pi$  as defined in Eq. (8). The light grey plain (dashed) curve (right vertical axis) is a section of the color plot for  $b_0 = 200$ , and  $\gamma_{31} = 0$  ( $\gamma_{31} = \gamma_{21}/1000$ ).

transparency is achieved before the pulse extinction. Considering a realistic experimental parameters for alkali metal atoms of  $b_0 = 200$ ,  $\gamma_{21} = 2\pi \times 6$  MHz, and  $\Omega_c = \gamma_{21}/2$ , the square pulse duration has to be longer than  $\tau_{EIT} \approx 21 \mu\text{s}$ . The homodyne measurement takes place within the decay time of the flash, typically  $\tau_f \sim 130$  ps, implying an unfavourably low duty cycle.

### 2.3. Square-pulse amplitude modulation

We now show that it is possible to improve the duty cycle by several orders of magnitude. To this end, we consider a periodic square-pulse amplitude modulation of the probe beam, with

$$E_i(t) = \begin{cases} 1, & -\frac{T}{2} < t < 0, \\ 0, & 0 \leq t \leq \frac{T}{2}, \end{cases} \quad (9)$$

and  $E_i(t + nT) = E_i(t)$  for all integers  $n$ . In Fig. 3, upper panel, we plot the transmitted intensity at the falling edge  $I(0^+)$  for  $b_0 = 200$  and  $\Omega_c = \gamma_{21}/2$ , in the 2D parameter space of pulse period  $T$  and probe detuning  $\delta_p$ . For the slow regime of  $T \gg \tau_{EIT}$ , the EIT steady state is achieved within the probe duration. The interference fringe pattern is independent of the modulation period and depends only on  $\Delta\Phi$  as given in Eq. (7). The same fringe pattern is also observed for  $T \ll \tau_{EIT}$ . In this case, as far as the EIT response of the medium is concerned, the probe beam can be considered as a time-averaged constant field with half amplitude. The resulting EIT field is also a constant field, with a phase shift of  $\phi_{EIT}$ . This is the basis for extending the self-aligned homodyne detection technique to higher modulation frequencies. Its performance at higher frequencies is summarized in the

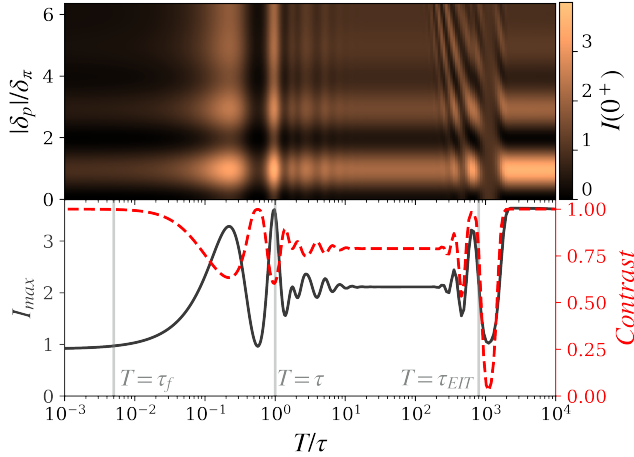


**Figure 3.** The upper panel shows  $I(0^+)$  as functions of the pulse period  $T/\tau$ , and probe detuning  $|\delta_p|/\delta_\pi$ . The lower panel shows the dependence of  $I_{\max}$  and fringe contrast on the pulse period. The parameters for the calculations are  $b_0 = 200$ ,  $\Omega_c = \gamma_{21}/2$  and  $\gamma_{31} = 0$ .

lower panel of Fig. 3, by the black curve for the maximum flash  $I_{\max}$  and the red dashed curve for the fringe contrast  $(I_{\max} - I_{\min})/(I_{\max} + I_{\min})$ .  $I_{\max}$  is defined as the intensity of the first fringe maximum of  $I(0^+)$ . The minimum intensity  $I_{\min}$  is found at resonance, where the destructive interference between  $E_s$  and  $E_{EIT}$  gives an anti-flash dip at the falling edge of the square pulse.

There are two regimes with unity contrast. The first one at  $T \gg \tau_{EIT}$  is the steady-state regime discussed previously. The second regime at  $T \ll \tau_f$  (i.e.,  $T/\tau \ll b_0^{-1}$ ) is of practical interest because of the much higher duty cycle. Due to the high modulation frequency, the sidebands are far-detuned and are transmitted unaffected through the atomic medium, summing up to an amplitude of  $E_i(t) - 1/2$ . Neglecting the off-resonance absorption in the transparency window, the transmitted carrier field amplitude is  $\exp(i\phi_{EIT})/2$ . As a result, the total transmitted signal is  $|E_i(t) + [\exp(i\phi_{EIT}) - 1]/2|^2$ , and retains the square-pulse shape. Some examples of the calculated transmitted signals at different  $\delta_p$  values are shown in the upper panel of Fig. 4. We observed a flip of the square pulse when  $|\delta_p|$  goes from zero to  $\delta_\pi$ , with a slight reduction of the signal due to the residual absorption. This signal, sensitive to the two-photon detuning, can be easily detected using standard amplitude-modulation spectroscopy. The fields decomposition of Eq. (6) can also be applied in this regime, noting that both the two-level and EIT responses of the atomic medium sees a “time-averaged” incident beam. As an example, we discuss the resonance case where  $E_s \approx -0.5$  and  $E_{EIT} \approx 0.5$ , giving  $I(t) \approx |E_i(t)|^2$ .

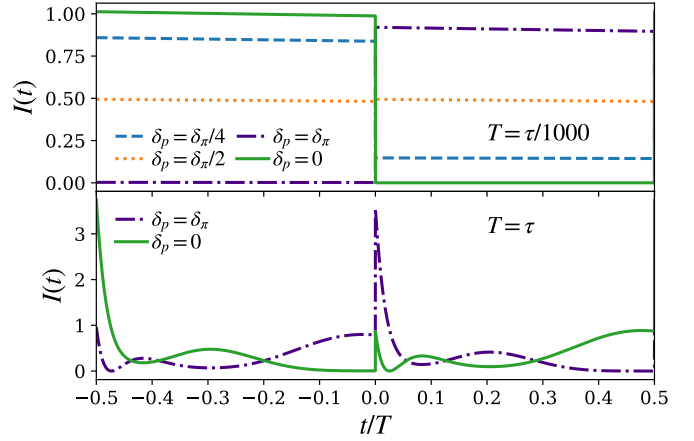


**Figure 4.** Transmitted signal for  $T < \tau_f$  (upper panel) and  $T > \tau_f$  (lower panel) at  $b_0 = 200$ ,  $\Omega_c = \gamma_{21}/2$  and  $\gamma_{31} = 0$ . The values of the modulation period and the two-photon detuning are given in the figure.

This can be easily extended to the case of  $\delta_p \neq 0$ .

To take advantage of the cooperative enhancement of the transient signals, we consider now the intermediate regime of  $\tau_f < T \lesssim \tau$ . While the duty cycle is still high, the modulation frequency is now long enough for the flashes to develop at both the leading and falling edges. At some modulation period, this leads to a higher  $I_{\max}$  (see lower panel of Fig. 4 for case of  $T\gamma_{21} = 1$ ). Here, the subsequent flash occurs during the transient of the previous flash. This leads to the oscillations in the values of  $I_{\max}$  and the contrast, as seen in lower panel of Fig. 3. This regime was previously studied in the two-level system [47]. Importantly, the contrast remains high for the cases where  $I_{\max}$  is maximal, making them useful for future applications.

## Conclusion

In conclusion, we have studied a new approach to determine the two-photon resonance frequency of an optically thick three-level  $\Lambda$ -system, in the transient regime. This technique is based on a self-aligned homodyne detection of the slow light of EIT through its interference with a flash. The latter is the fast cooperative emission of light after an abrupt extinction of the incident field, and has a time-scale that is well-separated from the EIT slow light. We showed that an amplitude-modulation spectroscopy with square pulse, allows a sensitive determination of the two-photon resonance, thanks to cooperative effects. This technique could be considered for CPT clocks [9], velocimetry [20] and magnetometry [55, 56] applications. Importantly, this technique can be performed in a wide range of modulation frequency that is higher than transition

linewidth, relying on a *time-averaged* regime of the EIT response. The optimum modulation frequency is a best compromise between the fast and the intermediate regime. In the fast regime, the transmitted signal retains its square-pulse profile, with unity contrast in the fringe pattern. The intermediate regime, on the other hand, benefits from the cooperative flash emission for larger signal amplitude. At the same time, the fringe contrast remains high.

The authors thank Thomas Zanon-Willette for critical reading of the manuscript. K.P. would like to acknowledge the funding from DST of grant No. DST/ICPS/QuST/Theme-3/2019. This work was supported by the CQT/MoE funding Grant No. R-710-002-016-271.

## Appendix

With a minor algebraic manipulation of Eq. (4) in main text, the susceptibility, for a weak probe beam of detuning  $\delta_p$  within the  $\Lambda$ -system in the steady-state regime, is given by,

$$\chi(\delta_p) = \frac{-6\pi\rho}{k^3} \frac{\frac{\gamma_{21}}{2} [\delta_p - \delta_c + \frac{i\gamma_{31}}{2}]}{(\delta_p + i\frac{\gamma_{21}}{2})(\delta_p - \delta_c + i\frac{\gamma_{31}}{2}) - \frac{|\Omega_c|^2}{4}}$$

For  $\delta_c = 0$ , the above expression reads,

$$\chi(\delta_p) = \frac{-6\pi\rho}{k^3} \frac{\frac{\gamma_{21}}{2} [\delta_p + \frac{i\gamma_{31}}{2}]}{\delta_p^2 - \frac{\gamma_{21}\gamma_{31}}{4} - \frac{|\Omega_c|^2}{4} + i\delta_p \frac{\gamma_{21} + \gamma_{31}}{2}}$$

In the limit of  $\gamma_{31}$  and  $\delta_p \ll \Omega_c$ ,  $\gamma_{21}$ , we can write,  $\delta_p^2 - \frac{\gamma_{21}\gamma_{31}}{4} - \frac{|\Omega_c|^2}{4} + i\delta_p \frac{\gamma_{21} + \gamma_{31}}{2} \approx -\frac{|\Omega_c|^2}{4} + i(\delta_p + i\frac{\gamma_{31}}{2})\frac{\gamma_{21}}{2}$ . Hence the expression for  $\chi$  can be written as

$$\chi(\delta_p) \approx \frac{-6\pi\rho}{k^3} \frac{\delta_p + \frac{i\gamma_{31}}{2}}{-\frac{|\Omega_c|^2}{4} - \frac{\gamma_{31}}{2} + i\delta_p}$$

Keeping to the first order in  $\delta_p$  and  $\gamma_{31}$ , we have

$$\chi(\delta_p) \approx \frac{6\pi\rho}{k^3} \frac{2\gamma_{21}}{|\Omega_c|^2} \left( \delta_p + i\frac{\gamma_{31}}{2} \right)$$

The real and the imaginary part of  $\chi$  can be written as follows:

$$\begin{aligned} \text{Re}\{\chi(\delta_p)\} &\approx \frac{6\pi\rho}{k^3} \frac{2\gamma_{21}}{|\Omega_c|^2} \delta_p, \\ \text{Im}\{\chi(\delta_p)\} &\approx \frac{6\pi\rho}{k^3} \frac{\gamma_{21}}{|\Omega_c|^2} \gamma_{31}. \end{aligned} \quad (.1)$$

We now derive the time delay. The group velocity,  $v_g$  the probe laser can be written as

$$v_g = \frac{c_0}{n(\omega_p) + \frac{\partial n}{\partial \omega_p} \omega_p}$$

where  $c_0$  is speed of light in vacuum,  $n = 1 + \text{Re}(\chi)/2$ ; Further we know that,  $n(\omega_p) \ll \frac{\partial n}{\partial \omega_p} \omega_p$  so  $v_g \approx \frac{c_0}{\frac{\partial n}{\partial \omega_p} \omega_p}$ .

Putting the value of the  $\text{Re}\{\chi\}$  from Eq. (.1) and using  $k = \omega_p/c_0$ , we get

$$n \approx 1 + \frac{1}{2} \frac{6\pi\rho c_0^3}{\omega_p^3} \frac{2\gamma_{21}}{|\Omega_c|^2} \delta_p \quad (.2)$$

where,  $\omega_0 = \frac{E_2 - E_1}{\hbar}$ . We remind the reader that  $\delta_p = \omega_p - \omega_0$ , so

$$\frac{\partial n}{\partial \omega_p} \approx \frac{1}{2} \frac{6\pi\rho c_0^3}{\omega_p^3} \left[ 1 - 3 \frac{\delta_p}{\omega_p} \right] \frac{2\gamma_{21}}{|\Omega_c|^2}$$

For the quasi-resonant case,  $\frac{\delta_p}{\omega_p} \ll 1$ , so the above equation becomes,

$$\frac{\partial n}{\partial \omega_p} \approx \frac{1}{2} \frac{6\pi\rho c_0^3}{\omega_p^3} \frac{2\gamma_{21}}{|\Omega_c|^2},$$

and the group velocity reads,

$$v_g \approx \frac{\omega_p^2}{6\pi\rho c_0^2} \frac{|\Omega_c|^2}{\gamma_{21}}. \quad (.3)$$

Finally, the time delay defined as  $\tau_{EIT} = L/v_g - L/c_0 \approx L/v_g$  is given by,

$$\tau_{EIT} \approx \frac{6\pi\rho c_0^2 L}{\omega_p^2} \frac{\gamma_{21}}{|\Omega_c|^2} = \frac{b_0 \gamma_{21}}{|\Omega_c|^2}. \quad (.4)$$

## References

- [1] G Alzetta, A Gozzini, L Moi, and G Orriols. An experimental method for the observation of rf transitions and laser beat resonances in oriented vapour. *Il Nuovo Cimento B* (1971-1996), 36(1):5–20, 1976.
- [2] K-J Boller, A Imamoglu, and S E Harris. Observation of electromagnetically induced transparency. *Physical Review Letters*, 66(20):2593, 1991.
- [3] E. Arimondo and G. Orriols. Nonabsorbing atomic coherences by coherent two-photon transitions in a three-level optical pumping. *Lettre al Nuovo Cimento* (1971-1985), 17(10):333–338, 1976.
- [4] L V Hau, S E Harris, Z Dutton, and C H Behroozi. Light speed reduction to 17 metres per second in an ultracold atomic gas. *Nature*, 397:594–598, 1999.
- [5] O Katz and O Firstenberg. Light storage for one second in room-temperature alkali vapor. *Nature Communications*, 9:2074, 2018.
- [6] F Bussi eres, N Sangouard, M Afzelius, H de Riedmatten, C Simon, and W Tittel. Prospective applications of optical quantum memories. *Journal of Modern Optics*, 60(18):1519–1537, 2013.
- [7] Y-F Hsiao, P-J Tsai, H-S Chen, S-X Lin, C-C Hung, C-H Lee, Y-H Chen, Y-F Chen, Ite A Yu, and Y-C Chen. Highly efficient coherent optical memory based on electromagnetically induced transparency. *Phys. Rev. Lett.*, 120:183602, May 2018.
- [8] A H Moustafa, L Xiaochi, G St ephane, C De Emeric, and B Rodolphe. A CPT-based cs vapor cell atomic clock with a short-term fractional frequency stability of  $3 \times 10^{-13} \tau^{-1/2}$ . *Journal of Physics: Conference Series*, 723:012013, jun 2016.

- [9] J Vanier. Atomic clocks based on coherent population trapping: a review. *Applied Physics B*, 81:421–442, 2005.
- [10] X Liu, E Ivanov, V I Yudin, J Kitching, and E A Donley. Low-drift coherent population trapping clock based on laser-cooled atoms and high-coherence excitation fields. *Phys. Rev. Applied*, 8:054001, 2017.
- [11] X Liu, J-M Mérolla, S Guérandel, C Gorecki, E de Clercq, and R Boudot. Coherent-population-trapping resonances in buffer-gas-filled cs-vapor cells with push-pull optical pumping. *Phys. Rev. A*, 87:013416, Jan 2013.
- [12] X Liu, V I Yudin, A V Taichenachev, J Kitching, and E A Donley. High contrast dark resonances in a cold-atom clock probed with counterpropagating circularly polarized beams. *Applied Physics Letters*, 111(22):224102, 2017.
- [13] F Ruihuan, H Chengyin, J Xunda, Q Yuxiang, G Yuanyuan, Z Minhua, H Jiahao, L Bo, and L Chaohong. Temporal spinwave fabry-perot interferometry via coherent population trapping. *arXiv:2008.12562*, 2020.
- [14] J A Sedlacek, A Schwettmann, H Kubler, R Low, T Pfau, and J P Shaffer. Microwave electrometry with rydberg atoms in a vapour cell using bright atomic resonances. *Nature physics*, 8:819, 2012.
- [15] D Shylla, E O Nyakang'o, and K Pandey. Highly sensitive atomic based mw interferometry. *Scientific Reports*, 8(1):8692, 2018.
- [16] C G Wade, M Marcuzzi, E Levi, J M Kondo, I Lesanovsky, C S Adams, and K J Weatherill. A terahertz-driven non-equilibrium phase transition in a room temperature atomic vapour. *Nature Communications*, 9:3567, 2018.
- [17] M Lam, S B Pal, T Vogt, M Kiffner, and W Li. Directional thz generation in hot rb vapor excited to a rydberg state. *Optics Letters*, 46(5):1017–1020, 2021.
- [18] A Aspect, E Arimondo, R Kaiser, N Vansteenkiste, and C Cohen-Tannoudji. Laser cooling below the one-photon recoil energy by velocity-selective coherent population trapping. *Physical Review Letters*, 61(7):826, 1988.
- [19] D Wilkowski, M Chalony, R Kaiser, and A Kastberg. Low- and high-intensity velocity selective coherent population trapping in a two-level system. *EPL (Europhysics Letters)*, 86(5):53001, jun 2009.
- [20] Z Chen, H M Lim, C Huang, R Dumke, and S-Y Lan. Quantum-enhanced velocimetry with doppler-broadened atomic vapor. *Phys. Rev. Lett.*, 124:093202, Mar 2020.
- [21] M Fleischhauer, A Imamoglu, and J P Marangos. Electromagnetically induced transparency: Optics in coherent media. *Rev. Mod. Phys.*, 77:633–673, Jul 2005.
- [22] A Tebben, C Hainaut, A Salzinger, S Geier, T Franz, T Pohl, M Gärtner, G Zürn, and M Weidemüller. Non-linear absorption in interacting rydberg eit spectra on two-photon resonance. *arXiv preprint arXiv:2102.11654*, 2021.
- [23] O Firstenberg, T Peyronel, Q-Y Liang, A V Gorshkov, M D Lukin, and V Vuletić. Attractive photons in a quantum nonlinear medium. *Nature*, 502(7469):71–75, 2013.
- [24] I Carusotto and C Ciuti. Quantum fluids of light. *Reviews of Modern Physics*, 85(1):299, 2013.
- [25] M Collombon, C Chatou, G Hagel, J. Pedregosa-Gutierrez, M Houssin, M Knoop, and C Champenois. Experimental demonstration of three-photon coherent population trapping in an ion cloud. *Phys. Rev. Applied*, 12:034035, Sep 2019.
- [26] C L Bentley, J Liu, and Y Liao. Cavity electromagnetically induced transparency of driven-three-level atoms: A transparent window narrowing below a natural width. *Phys. Rev. A*, 61:023811, Jan 2000.
- [27] H Wang, D J Goorskey, W H Burkett, and M Xiao. Cavity-linewidth narrowing by means of electromagnetically induced transparency. *Opt. Lett.*, 25(23):1732–1734, Dec 2000.
- [28] M D Lukin, M Fleischhauer, M O Scully, and V L Velichansky. Intracavity electromagnetically induced transparency. *Opt. Lett.*, 23(4):295–297, Feb 1998.
- [29] H Gessler, Z Jiepeng, and Yifu Z. Vacuum rabi splitting and intracavity dark state in a cavity-atom system. *Phys. Rev. A*, 76:053814, Nov 2007.
- [30] H Wu, J Gea-Banacloche, and M Xiao. Observation of intracavity electromagnetically induced transparency and polariton resonances in a doppler-broadened medium. *Phys. Rev. Lett.*, 100:173602, May 2008.
- [31] M D Lukin, M Fleischhauer, A S Zibrov, H G Robinson, V L Velichansky, L Hollberg, and M O Scully. Spectroscopy in dense coherent media: Line narrowing and interference effects. *Phys. Rev. Lett.*, 79:2959–2962, 1997.
- [32] A Godone, F Levi, S Micalizio, and J Vanier. Dark-line in optically-thick vapors: inversion phenomena and line width narrowing. *Eur. Phys. J. D*, 18(1):5–13, Jan 2002.
- [33] C C Kwong, T Yang, M S Pramod, K Pandey, D Delande, R Pierrat, and D Wilkowski. Cooperative emission of a coherent superflash of light. *Phys. Rev. Lett.*, 113:223601, Nov 2014.
- [34] J E Thomas, P R Hemmer, S Ezekiel, C C Leiby, R H Picard, and C R Willis. Observation of ramsey fringes using a stimulated, resonance raman transition in a sodium atomic beam. *Phys. Rev. Lett.*, 48:867–870, 1982.
- [35] G S Pati, K Salit, R Tripathi, and M S Shahriar. Demonstration of raman-ramsey fringes using time delayed optical pulses in rubidium vapor. *Optics Communications*, 281(18):4676 – 4680, 2008.
- [36] T Zanon, S Guérandel, E de Clercq, D Holleville, N Dimarcq, and A Clairon. High contrast ramsey fringes with coherent-population-trapping pulses in a double lambda atomic system. *Phys. Rev. Lett.*, 94:193002, May 2005.
- [37] K A Barantsev, E N Popov, and A N Litvinov. Line shape of coherent population trapping resonance in the  $\lambda$ -scheme under ramsey-type interrogation in an optically dense medium. *Quantum electronics*, 48(7):615, 2018.
- [38] L Nicolas, T Delord, P Jamonneau, R Coto, J Maze, V Jacques, and G Hétet. Coherent population trapping with a controlled dissipation: applications in optical metrology. *New Journal of Physics*, 20(3):033007, 2018.
- [39] D Wei, J F Chen, M M T Loy, G K L Wong, and S Du. Optical precursors with electromagnetically induced transparency in cold atoms. *Phys. Rev. Lett.*, 103:093602, Aug 2009.
- [40] V M Datsyuk, I M Sokolov, D V Kupriyanov, and M D Havey. Diffuse light scattering dynamics under conditions of electromagnetically induced transparency. *Phys. Rev. A*, 74:043812, Oct 2006.
- [41] A Sommerfeld. Über die fortpflanzung des liches in disperdierenden medien. *Ann. Phys. (Leipzig)*, 44(177), 1914.
- [42] L Brillouin. Über die fortpflanzung des licht in disperdierenden medien. *Ann. Phys. (Leipzig)*, 44(204), 1914.
- [43] Q-Q Bao, B Fang, X Yang, C-L Cui, and J-H Wu. Marking slow light signals with fast optical precursors in the regime of electromagnetically induced transparency. *J. Opt. Soc. Am. B*, 31(1):62–66, Jan 2014.
- [44] Y D Peng, A H Yang, B Chen, Y Xu, and L Y Zhang. Magnetically induced separation and enhancement of optical precursors via electromagnetically induced transparency. *The European Physical Journal D*, 66:296, 2012.
- [45] N Bloembergen, E M Purcell, and R V Pound. Relaxation effects in nuclear magnetic resonance absorption. *Phys. Rev.*, 73:679–712, Apr 1948.

- [46] K Toyoda, Y Takahashi, K Ishikawa, and T Yabuzaki. Optical free-induction decay of laser-cooled  $^{85}\text{Rb}$ . Phys. Rev. A, 56:1564–1568, Aug 1997.
- [47] C C Kwong, T Yang, D Delande, R Pierrat, and D Wilkowski. Cooperative emission of a pulse train in an optically thick scattering medium. Phys. Rev. Lett., 115:223601, Nov 2015.
- [48] M Chalony, R Pierrat, D Delande, and D Wilkowski. Coherent flash of light emitted by a cold atomic cloud. Phys. Rev. A, 84:011401, Jul 2011.
- [49] J D Jackson. Classical electrodynamics. Wiley, New York, 3rd ed. edition, 1999.
- [50] C C Kwong, E A Chan, S A Aljunid, R Shakhmuratov, and D Wilkowski. Large optical depth frequency modulation spectroscopy. Opt. Express, 27(22):32323–32336, Oct 2019.
- [51] S Brandt, A Nagel, R Wynands, and D Meschede. Buffer-gas-induced linewidth reduction of coherent dark resonances to below 50hz. Phys. Rev. A, 56:R1063–R1066, Aug 1997.
- [52] M A Bouchiat and J Brossel. Relaxation of optically pumped Rb atoms on paraffin-coated walls. Phys. Rev., 147:41–54, Jul 1966.
- [53] M T Graf, D F Kimball, S M Rochester, K Kerner, C Wong, D Budker, E B Alexandrov, M V Balabas, and V V Yashchuk. Relaxation of atomic polarization in paraffin-coated cesium vapor cells. Phys. Rev. A, 72:023401, Aug 2005.
- [54] M Klein, M Hohensee, D F Phillips, and R L Walsworth. Electromagnetically induced transparency in paraffin-coated vapor cells. Phys. Rev. A, 83:013826, Jan 2011.
- [55] M Fleischhauer, A B Matsko, and M O Scully. Quantum limit of optical magnetometry in the presence of ac Stark shifts. Phys. Rev. A, 62:013808, Jun 2000.
- [56] D Budker, W Gawlik, D F Kimball, S M Rochester, V V Yashchuk, and A Weis. Resonant nonlinear magneto-optical effects in atoms. Rev. Mod. Phys., 74:1153–1201, Nov 2002.